IEEE Access
Multidisciplinary | Rapid Review | Open Access Journal

Received April 19, 2022, accepted May 4, 2022, date of publication May 9, 2022, date of current version May 12, 2022.

Digital Object Identifier 10.1109/ACCESS.2022.3173422

Transient Stability Enhancement Through Individual Machine Equal Area Criterion Framework Using an Optimal Power Flow

SREENADH BATCHU AND KIRAN TEEPARTHI, (Member, IEEE)
Department of Electrical Engineering, NIT Andhra Pradesh, Tadepalligudem 534101, India
Corresponding author: Kiran Teeparthi (kiran.t39@nitandhra.ac.in)

ABSTRACT Preventive control actions for enhancing the transient stability of power system ensures the system stability under a given contingency. Generation rescheduling through stability constrained optimal power flow (TSC-OPF) is one of the widely adopted preventive control scheme. This study reports an approach for enhancement of transient stability using global transient stability constrained optimal power flow (TSC-OPF) methods. The proposed approach uses individual machine equal area criterion framework (IMEAC), which is a direct time-domain approach for transient stability analysis, to carry out two important functional aspects of TSC-OPF methods: first, individual machine Kimbark curves (IMKC) are used to perform the transient stability analysis; second, IMKC around the critical clearing time (CCT) are used to identify most severely disturbed machines (MDM) for the given contingency. Further, the critical trajectories of these MDMs are utilized in forming reference transient stability constraints, at only one particular time step of integration. In such manner, transient stability constraints are modified at each iteration of TSC-OPF, so that they represent the dynamic response of the power system efficiently, while operating condition is improving through TSC-OPF iterations. Numerical examples demonstrate the effectiveness and main properties of the proposed approach.

INDEX TERMS Critical trajectory, dynamic liberation point, individual machine Kimbark curve, leading loss of synchronism point, most severely disturbed machines, transient stability constraints, transient stability constrained optimal power flow.

I. INTRODUCTION

TSC-OPF is an useful tool to determine optimal generation reschedule, while ensuring power system stability after a large disturbance. It is a nonlinear optimization problem with several nonlinear constraints and variables [1]. One of the main approaches to solve TSC-OPF is numerical optimization approach [2]. In [3] and [4] a constraints transcription based numerical optimization approach is presented, in which infinite dimensional TSC-OPF problem was converted into to solvable finite dimensional problem. In this approach number of optimization variables are remains same as that of conventional OPF. However, with this approach, it is not possible to observe dynamic variables temporal behaviour. As a second approach, in [5], a simultaneous desctretization method is proposed, in which dynamic constraints are converted into numerically equivalent algebraic constraints and included into the OPF problem. Some key questions that need to be addressed while implementing this approach are: (i). How to determine the transient stability index (TSI) such that the system can be brought back from vulnerable state to a secure state under a given contingency. (ii). What is the efficient way of forming stability constraints so that number of non linear constraints gets reduced. (iii). How to select the solution period for which TSC-OPF must be solved so that computational burden gets reduced. Several methods have been investigated and proposed by the researchers to answer questions (i),(ii), and (iii). In [5] a TSI based on heuristic rotor angle limits is proposed, and [6], [7], [10] adopted the same rotor angle based TSI. The main limitation of such a TSI is the heuristically chosen rotor angle limit. If, the chosen rotor angle limit is a small value (lets say 90°) then operation of the system will be pushed towards more secure and sub optimal. On the other hand, a high value

The associate editor coordinating the review of this manuscript and approving it for publication was Siqi Bu.

relax the stability constraint too much and may results in an insecure or critically secure operation. In addition, the number of transient stability constraints to be incorporated in TSC-OPF is equal to the number of solution time steps taken into account for dynamic constraints multiplied by the total system generators, *Ng*. In [11], TSI based on the dot product criterion of generator rotor angle trajectories was used and formulated the corresponding transient stability constraints(TSC). The number of TSC in this method are same as that of TSC-OPF solution time steps. However, with respect to solution interval of the TSC-OPF, this approach employed an arbitrary end time. A TSC-OPF considering complete system simulation model and a generator speed COI based TSI is adopted in [8], [9], but with an arbitrary solution interval for TSC-OPF. An adaptive TSI, relying on the maximum rotor angle limit of single machine equivalent (SIME) of multi machine system is proposed [12]. TSI is adjusted iteratively until the required stabilization is achieved. In [5], [11], [12] the solution interval for TSC-OPF is determined heuristically, which has the effect of increased computational burden. Another SIME based approach for transient stability enhancement is proposed in [13]. This method is considered as a major break through in forming TSC for global TSC-OPF, because TSC in this method are reduced to just single constraint and the end time limit for solution period of TSC-OPF is selected non-heuristically using the time to instability of SIME trajectory, so that solution interval is no more unpredictable or unnecessarily large. In [15], power system kinetic energy based TSC is formulated to deal with extremely unstable conditions through TSC-OPF. However, as the SIME method is based on compressing the multiple machine dynamics into two machine equivalent and then to one machine equivalent. This non linear conversion process introduces non negligible approximations and errors. Further, SIME represents aggregated effect of critical machines motion with respect to non critical machines motion. By this aggregation process, the observation of individual machine rotor angle dynamics of motion is no longer available to operator. Also, dedicated software are needed to carryout SIME related calculations from the multi machine time domain simulations. However, apart from their limitations, indeed all the above main stream methods where TSC are expressed in interms of rotor angle deviations offered a significant progress in methods for enhancing the transient stability through global TSC-OPF methods. An alternative method for solving TSC-OPF is proposed in [16], where in TSC are expressed as CCT of the given contingency, and this CCT values are estimated using artificial neural networks (ANN).

Transient stability analysis (TSA) from the sense of individual machines provides unique approach as in these methods stability analysis is carried out using the motion of only some individual critical machines [17], [18]. Hence, individual machine based methods has been selected to reach the goal of this study. Ref. [19] proposes a TSA technique based on individual machine energy functions.. A detailed machine by machine analysis is performed in [20], [21], and introduced the concept of individual machine partial energy function (PEF). Recently, [22]–[25] developed a unique individual machine kimbark curve (IMKC) based framework and a parallel monitoring technique based on IMKC for TSA under a given contingency. In [26], a detailed theoretical framework is offered that explains the relation between transient trajectory of the system and energy conversion in the individual machine. A transient stability enhancement scheme based on individual machine methods has been presented in [27], however, in this paper transient stability constraints are included at all time steps of TSC-OPF solution and solution interval is determined using an empirical relation obtained from the critical trajectories of individual machines which in general is more than the time to instability of system, and hence adds to the computational burden of TSC-OPF.

Motivated from the concepts of transient stability assessment (TSA) using individual machine equal area criterion (IMEAC) presented in [22]–[26], the authors of the paper [27] first time attempted to develop a workflow for transient stability control through IMEAC framework, which opened a further research direction for potentially utilizing this well-developed theory of IMEAC based TSA. In the initial research presented in [27], the authors concluded that (i). The necessary and sufficient condition on number of individual machines whose transient stability constraints must be included into TSC-OPF formulation to ensure transient stability is equal to number of most disturbed machines (MDMs) and these transient stability constraints are included at all time steps of solution interval (ii). The empirical time interval for which TSC-OPF needs to be solved to ensure transient stability under a given contingency is, t_{end}^{emp}, which is derived from the critical rotor angle trajectories of MDMs at initial operating point (iii). A security-based severity index (γ_{MDM}) is introduced to achieve a smooth reconciliation between transient security level versus generation operation cost. Further, conclusion section in [27], also shows a research scope for (a). reducing the number of transient stability constraints which can be imposed on MDMs to a minimum number (b). Identifying the minimum deterministic time interval in terms of IMEAC, which further can be utilized as a necessary integration interval for which dynamic constraints needs to be incorporated into TSC-OPF formulation. Ref. [13], is an important paper in the field of TSC-OPF research, in which the authors for the first time reported a non-heuristic way of forming transient stability constraints in TSC-OPF, and number of transient stability constraints are simply reduced to only one. Further, a deterministic time interval in terms of time to instability of single machine equivalent (SIME) trajectory of multi machine system, for which TSC-OPF needs to be solved for ensuring first swing stability is also proposed. Hence, To answer the research scope given by [27] to some extent, present paper attempts to effectively integrate the procedures of [13] and [27] to come up with a improved method over these parental techniques for securing the transient stability under a given contingency.

A. OBJECTIVES AND CONTRIBUTIONS

The objective of this paper is to answer the questions (i), (ii), and (iii) from an individual machine perspective without resorting to any multi machine to SIME kind of transformations. The next questions raised from this objective are a).Which individual machine trajectories are best suited to form a TSI, so that the insecure system can be bring back to secure state b). How to form an accurate and effective TSC in terms of individual machines so that number of constraints gets reduced c). What is the way of choosing a non-heuristic TSC-OPF solution interval limit in terms of these individual machine trajectories. Ref. [27] tries to answer the above objectives to an extent. But,answering, the above questions in an alternative way from the individual machine perspective not only forms a new approach but also contributes to the knowledge of application of individual machine methods in transient stability control applications. The following are the primary contributions of this work:

(i). Unlike [27], having a contingency scenario in hand to stabilize, TSC that are needed to be included into TSC-OPF are decreased to only number of most severely disturbed machines (MDM). Further, unlike [13], this process does not need any multi machine to one machine equivalent transformations for reducing the number of TSC.

(ii). This constraint are included in TSC-OPF formulation at only one time step of integration, called time to leading out of step point, t_{LOSP}, which is calculated from kimbark curves of individual machines.

(iii). The solution interval during which dynamic and transient constraints must be considered in the TSC-OPF formulation is defined from t_0 to t_{LOSP}, so that the problem dimension is adjusted according to time to instability, t_{LOSP}, instead of choosing an arbitrary solution interval.

(iv). The transient stability index value to maintain the synchronism is furnished according to the critical trajectory (i.e trajectory corresponding to critical clearing time) of MDM, which eliminates the usage of heuristic limits.

Critical machines are defined in this research as machines having advanced rotor angles in the post-fault scenario [17], [18]. The test system (TS) is based on a IEEE 39 bus system [28], [29], with the inertia constant of the generator at bus 39 reduced from 500 p.u to 100 p.u.. [22]. All faults are of type three phase to ground fault applied at $t_0 = 0$ s and cleared after a time t_{cl} s with or without line trip. A notation used in [22] is adopted to indicate the contingency type. For example a contingency representation [TS, bus 11, 400 ms] indicates that a three phase to ground fault is occurred in test system at bus 11 and cleared after 400 ms without tripping any line. In the same way representation [TS, bus 11, 400 ms line11-16] indicates that a three phase to ground fault bus 11 and cleared after 400 ms with the tripping of the line connected between buses 11 and 16. The bus number to which a machine in the test system is connected is used to identify that machine. For example, notation, machine-32, refers to the generator attached to bus 32 in the TS. Further, the novelty of this study lies in exploring the potential of the IMEAC theory in reducing the number of transient stability constraints in TSCOPF to just the number of most disturbed machines and expressing the minimum solution interval for which TSC-OPF needs to be solved in terms of equal area criterion of individual machines while stabilizing a given contingency.

B. ORGANIZATION OF THE PAPER

The rest of the paper is laid out as follows: Section II briefly reviews the global TSC-OPF formulation. Section III reviews the important theory and concepts related to TSA using individual machine kimbark curve frame work. Formulation of the proposed transient stability constraint and transient stability control algorithm is presented in Section IV. Numerical example illustrating the proposed approach is presented in Section V. Proposed method is compared with existing approaches in Section VI. Discussion on some aspects of the proposed method with respect to previous research in [27] is presented in Section VII. Finally, conclusions are presented in Section VIII.

II. GLOBAL TSC-OPF: PROBLEM FORMULATION

TSC-OPF is an useful tool to determine optimal generation reschedule, while ensuring power system stability after a large disturbance. It considers both static and dynamic constraints while optimizing the operating variables. Mathematical formulation of TSC-OPF from the inception of the disturbance at time t_0 s to disturbance clearing time t_{cl} s and to the end of simulation time t_{end}, $T = [t_0, t_{cl}) \cup (t_{cl}, t_{end}]$, considering the classical generator model, can be expressed as follows [13]:

$$min\, f(P_{Gi}) = \sum_{i=1}^{N_g} a_i + b_i P_{gi} + c_i (P_{gi})^2 \tag{1}$$

$$\text{subjected to } P_{gi} - P_{li} = \sum_{j \in i} P_{ij}(V, \theta) \tag{2a}$$

$$Q_{gi} - Q_{li} = \sum_{j \in i} Q_{ij}(V, \theta) \tag{2b}$$

$$E_i V_i^0 \sin(\delta_i^0 - \theta_i^0) = X_{di}^{'} P_{gi} \tag{2c}$$

$$E_i V_i^0 \cos(\theta_i^0 - \delta_i^0) - (V_i)^2 = X_{di}^{'} Q_{gi} \tag{2d}$$

$$\omega_i^0 - \omega_s = 0 \tag{2e}$$

$$V_i^{min} \le V_i \le V_i^{max} \tag{2f}$$

$$P_{gi}^{min} \le P_{gi} \le P_{gi}^{max} \tag{2g}$$

$$Q_{gi}^{min} \le Q_{gi} \le Q_{gi}^{max} \tag{2h}$$

$$E_i^{min} \le E_i \le E_i^{max} \tag{2i}$$

$$\delta_i^{t+1} - \delta_i^t = \frac{\Delta t}{2} \left(\omega_i^{t+1} - \omega_i^t - 2\omega_s \right) \tag{2j}$$

$$\omega_i^{t+1} - \omega_i^t = \frac{\Delta t}{2M_i} \left(2P_m - P_{ei}^{t+1} - P_{ei}^t \right) \tag{2k}$$

$$\left| \delta_{i,COI}^t \right| \le K \tag{2l}$$

where, f(.) is the total generation cost function.Eqs. (2a)-(2b) represents steady state power flow constraints at each bus. Eqs.(2c)-(2e) represents constraints on generator state variables initial conditions. Eq. (2f) represents constraints on system bus voltages. Eqs. (2g)-(2h) represents constraints on generating unit active reactive power capabilities. Eqs. (2j)-(2k) represents dynamic constraints formed as a difference constraints from the swing equation at a generic time step t, using the trapezoidal rule. Eq.(2l) represents the transient stability constraint (TSC), which forces the all rotor angles to be within the limit K, during entire solution interval. Formulation of the proposed transient stability constraint is discussed in section IV-A. The novelty of the proposed TSC consists in its formulation based on the individual machine equal area criterion (IMEAC) and rotor angle trajectories of class of individual machines called most severely disturbed machines (MDM). Unlike the method discussed in [13], proposed method does not need any equivalent trajectory of multi machine system to form required constraints. The basics of transient stability assessment under IMEAC frame work are discussed in section III.

III. PRINCIPLES OF THE INDIVIDUAL MACHINE EQUAL AREA CRITERION (IMEAC) METHOD

IMEAC method is a direct time domain method, which analyzes the system trajectory of a multi machine system from the perspective of individual machine power-vs-angle curve. In IMEAC method [22], [23], an ''individual machine'' is represented as ''individual machine'' in COI reference (i.e, rotor angle motion of each individual machine i is refered with respect to system COI). As a result, system COI can be viewed as a virtual ''machine,'' with its own equation of motion expressed as the combined motion of all the machines in the system. Because machine i and COI are viewed as two ''individual machines'' with interactions, a two-machine system is created by combining individual machine-virtual COI machine pairings (IVCS). As is generally known, the equal area criteria (EAC) is only applicable in the one machine-infinite bus system (OMIB) and the two machine system. However, because the IVCS constitutes precisely two machine system, EAC can also be applied to an individual machine. The rotor angle of machine i, which is referred with respect to the virtual COI machine, can be written as follows:

$$\begin{aligned} \dot{\theta}_i &= \tilde{\omega}_i \\ M_i\dot{\tilde{\omega}}_i &= f_i \end{aligned} \tag{3}$$

where, $f_i = P_{mi} - P_{ei} - \frac{M_i}{M_T}P_{COI}$; $\theta_i = \delta_i - \delta_{COI}$; $\tilde{\omega} = \omega_i - \omega_{COI}$; $P_{COI} = \sum_{i=1}^{n}(P_{mi} - P_{ei})$; $\delta_{COI} = \frac{1}{M_T}\sum_{i=1}^{n} M_i\delta_i$; $\omega_{COI} = \frac{1}{M_T}\sum_{i=1}^{n} M_i\omega_i$; The Kimbark curve is the power-angle relationship of i^{th} machine evaluated in θ_i-f_i space. The following are two key conclusions about the Kimbark curve of a single machine:

(i). The Kimbark curve of a critical machine (CM) has strong acceleration-deceleration features. As a result, the equal area criterion (EAC) strictly applicable to critical machines.

(ii). A non critical machine (NCM) is one that is only little affected by a fault, and so does not have strong acceleration-deceleration patterns in its Kimbark curve.

Because EAC exclusively holds for critical machine, a dynamic liberation point (DLP) appears on the Kimbark curve of an unstable critical machine. On the Kimbark curve of a stable critical machine, there occurs a dynamic stationary point (DSP). As a result, the stability of an individual machine is evaluated based on the existence of either DLP or DSP on its Kimbark curve. Further, the unity principle establishes a link between the stability of individual machine and the stability of the entire system [22]. According to it, a multi-machine system is declared as:

(i). Transiently stable if all critical machines post fault Kimbark curves exhibits only DSPs on them, no DLPS.

(ii). Transiently unstable if there occurs at least one DLP on kimbark curves of the critical machines.

Eq.(4a) gives the stability margin (η_i) of an unstable critical machine, while Eq. (4b) gives the stability margin (η_i) of a stable critical machine.

$$\eta_i = (A_{DECi} - A_{ACCi})/A_{ACCi} \tag{4a}$$

$$\eta_i = (A_{DECi} + A_{DECi}^{EXT} - A_{ACCi})/A_{ACCi} \tag{4b}$$

where, A_{DECi} and A_{ACCi}, represents acceleration and deceleration areas on corresponding Kimbark curve of i^{th} machine. According to IMEAC, the system is judged as transiently stable if $\eta_i > 0$ (i,e, rotor angle trajectory of CM is bounded w.r.t time and there occurs only DSPs on corresponding kimbark curves of CMs) unstable if $\eta_i < 0$ (i,e, rotor angle trajectory of CM is unbounded w.r.t time, and there occurs at least one DLP on corresponding kimbark curves of CMs), and critically stable if $\eta_i = 0$ (i.e, rotor angle trajectory of CM reaches its critical trajectory). A CM with lowest stability margin is considered as most severely disturbed machine (MDM).

$$\eta_{MDM} = min\,[\eta_i] \quad i \in \Gamma_c \tag{5}$$

where, Γ_c is the set having all the critical machines. The concept of MDM is very much useful in TSA using IMEAC because the system stabil status can be reflected completely by the MDM stability status. If MDM is stable, the system is stable; if MDM is unstable, the system is unstable; and if MDM is critically stable, the system is critically stable. In [23], a method for determining MDMs for the given fault scenario is proposed, which examines individual machine margins around critical clearing time. A qualitative approach of the same method is adopted in this paper to determine MDMs under the given fault scenario.

To illustrate the TSA using individual machine kimbark curves, consider a representative fault scenario [TS, bus-11, line 11-6]. This scenario involves a three-phase ground fault at bus 11, which is cleared by tripping the line connecting

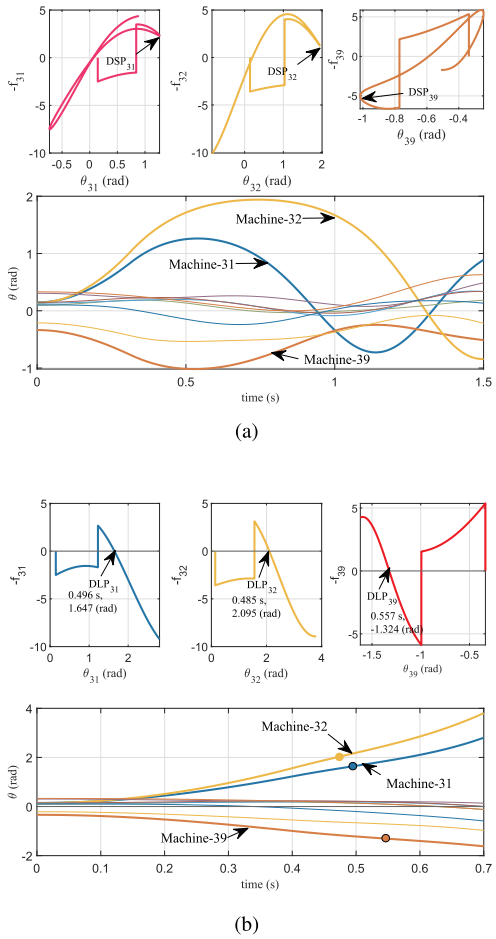

FIGURE 1. Kimbark curves and rotor angle deviations w.r.t COI for (a) a stable scenario [TS, bus-11, 314 ms line 11-6] (b) an unstable scenario [TS bus-11, 400 ms, line 11-6] .

buses 11 and 16. The rotor angle profiles for the fault duration of 314 ms are shown in Fig. 1(panel(a)). From the figure it can be observed that machine-31, 32 and 39 exhibits advanced rotor angle in the post fault system trajectories and hence considered as a critical machines (CM). Corresponding Kimbark curves also shows only DSPs on them, which represents that all CM are stable and hence system stability status can be declared as stable. Fig.1(panel(b)) shows the plots for the fault duration of 400 ms. In this case there occurs DLP on each individual CM kimbark curve. Further, it is interesting to note that DLP of each machine is occurring at different instances along the time horizon. For example DLP of machine -31 occurs at 0.496 s, machine-32 occurs at 0.485 s and machine-39 occurs at 0.557 s. According to the unity principle, if at least one DLP appears on post-fault Kimbark curves, the system is considered transiently unstable. According to nomenclature of IMEAC the DLP of individual machine is termed as loss of synchronism point (LOSP) or out of step point, LOSP which occurs first along the time horizon is termed as ''leading LOSP,'' and the time at which this point occurs is denoted as time to leading LOSP, t_{LOSP}. For the case in hand, leading LOSP occurs on machine-32, with $t_{LOSP} = 0.485$ s.

Now, to determine most disturbed machines (MDMs) for the given contingency, observe the behaviour of the kimbark curves (KC) of CMs in the neighbourhood of its CCT. For a representative example consider the same case [TS, bus-11, line 11-6]. For the current scenario, the CCT is 316 ms, and the Kimbark curves of CMs around CCT are shown in Fig.2. Kimbark curves of Case-A are pertaining to scenario that is stable, Case-B for a scenario that is critically stable and Case-C for a scenario that is critically unstable. From the figure it is interesting to note that, in all the cases Machine-31 and 39 KCs shows only DSPs on them irrespective of system stability status. But, KC of machine-32 shows DSP when system is stable ([TS, bus-11, 315 ms, line 11-6]), CDSP when the system us critically stable ([TS, bus-11, 316 ms, line 11-6]), and DLP when the system is critically unstable ([TS, bus-11, 317 ms, line 11-6]). It leads to the key conclusion that the whole information about the system's critical stability for the scenario [TS, bus-11, line 11-6] is incorporated in the machine-32's stability. In other words, for the fault scenario in hand the instability of the system originates from the instability of machine-32. The suggested method is novel in that, it allows for the formation of transient stability constraints in the global TSC-OPF, utilising the critical trajectory of this MDM, to ensure the transient stability under the given contingency. The next section will go through this in detail.

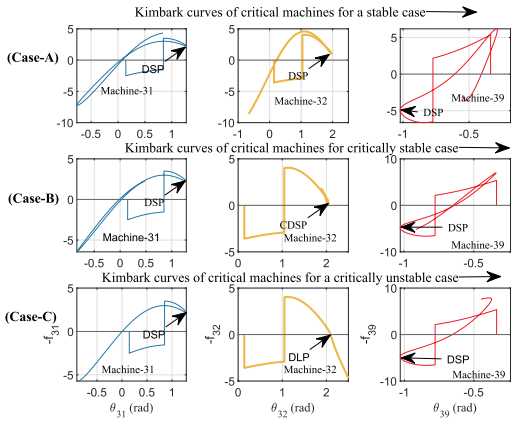

FIGURE 2. CM Kimbark curves around the CCT of the given contingency; Case-A: A scenario that is stable [TS, bus-11, 315 ms, line 11-6], Case-B: A scenario that is critically stable case [TS, bus-11, 316 ms, line 11-6], Case-C: A scenario that is critically unstable case [TS, bus-11, 317 ms, line 11-6].

IV. PROPOSED TSC-OPF APPROACH USING IMEAC

In this section a new approach for enhancing transient stability under a given contingency using TSC-OPF through IMKC theory of TSA is proposed. Proposed approach reduces the number of transient stability constraints (TSC) to just the number of most disturbed machines (N_MDM). Additionally, the solution period of TSC-OPF, $T = [t_0, t_{cl}) \cup (t_{cl}, t_{end}]$,

is limited and chosen non heuristically to a value called time to leading LOSP ($t_{end} = t_{LOSP}$), which is obtained from the Kimbark curves of individual machines. The new proposed TSC and its formulation using the MDM critical trajectories is presented in the following discussion.

A. PROPOSED TRANSIENT STABILITY CONSTRAINT FORMULATION

Given an unstable contingency at the initial operating (IOP) point, the stabilization process needs to improve the IOP such that critical machine Kimbark curves shows only DSPs for this contingency. In other words, the IOP should be modified in such a way that CCT at new operating point (OP) must be greater than equal to actual fault clearing time of the contingency. Also, as discussed in the previous section, at an operating point critical instability of the system originates from the instability of MDM. So given an unstable contingency, if MDM trajectories at this fault clearing time are constrained below their critical trajectories, the system stability is ensured for the given scenario.

From the IOP and contingency scenario, evaluate the individual machine Kimbark curves, to calculate time to leading LOSP, t_{LOSP}, and MDM for the given scenario, considering the original fault clearing time and the evaluated critical clearing time, respectively. Fig. 3 shows a representative transient evolution of an unstable and critically stable MDM trajectories for the scenario [TS, bus-11, line 11-16]. It is well known form the concepts of transient stability that critical trajectory of MDM (i.e, δ_{CTMDM}) is always lower than corresponding unstable trajectory (δ_{UTMDM}), as shown in 3, where, $\delta_{CTMDM}(t_{LOSP})$ and $\delta_{UTMDM}(t_{LOSP})$ are the rotor angles at t_{LOSP} on stable and unstable trajectories, respectively.

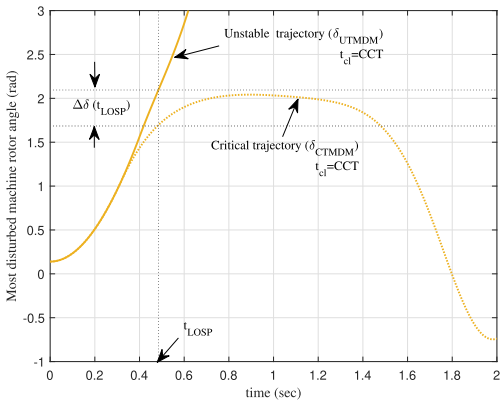

FIGURE 3. A representative unstable and critical trajectories of MDM for the scenario [TS, bus-11, line 11-16]: machine-32 is MDM and t_{LOSP}=0.485 s.

The degree of instability can be reduced by carrying out the stabilization procedure at t_{LOSP}, which is the time at which multi machine system is assessed transiently unstable. At this time, the multi machine system can be made stable by constraining all MDM rotor angle trajectories within the corresponding critical trajectories. Based on this observation, it is put forward to set the the angular deviation of MDM at LOSP (i.e., $\Delta\delta_{MDM}(t_{LOSP}) = \delta_{UTMDM}(t_{LOSP} - \delta_{CTMDM}(t_{LOSP}))$ to zero. Rested up on this formulation, the TSC can be set as follows:

$$|\delta_{UTMDM}(t_{LOSP}) - \delta_{CTMDM}(t_{LOSP})| \leq K_h \quad (6a)$$

$$\Delta\delta_{MDM}(t_{LOSP}) \leq K_h \quad (6b)$$

where, K_h is the required deviation threshold in the order of 10^{-4}, and $\Delta\delta_{MDM}(t_{LOSP})$ is a single scalar value at t_{LOSP}. Having defined the transient stability constraint, the transient stability at initial operation point can be improved by solving the global TSC-OPF formulated using Eqs.(1)-(2k) and Eq.(6b), which provides a new improved operating point with respect to transient stability. However, because the MDM critical trajectory accurately reflects the rotor angular deviation only at the original operating point, not at the new operating point (OP), obtained after solving TSC-OPF, complete stabilisation of the given contingency may not be achieved. Hence, in order to confirm system stability at the new OP, a transient stability assessment must be repeated at this new OP. As long as system is transiently unstable, it is necessary to determine the critical trajectory for the new OP for updating the TSC in Eq.(6b), so that the updated TSC can be incorporated into the next TSC-OPF solution procedure.

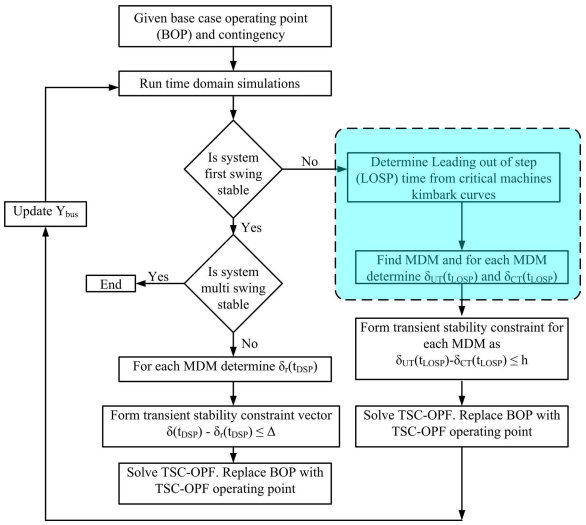

FIGURE 4. Proposed algorithm flow chart.

Fig.4 shows the flow chart for the proposed algorithm. The description of flow chart for transient stability enhancement is given below:

step 1: Start with a base case operating point (BOP).

step 2: For the given fault scenario, run time domain simulations, evaluate individual machine kimbark curves and assess the transient stability of the system using IMEAC. If system is first swing unstable go to step 3 else go to step 6.

step 3: Determine the leading out of step time,t_{LOSP}, and find most severely disturbed machines (MDM) and

TABLE 1. Generation schedule at IOP for [TS, bus-11, 400 ms].

Unit No	Power (MW)	Unit No	Power (MW)
Machine- 30	243.79	Machine- 35	649.16
Machine- 31	564.65	Machine- 36	557.41
Machine- 32	639.05	Machine- 37	536.20
Machine- 33	628.55	Machine- 38	831.53
Machine- 34	507.46	Machine- 39	983.19

their critical trajectories. Derive the the parameter $\delta_{CTMDM}(t_{LOSP})$.

step 4: Form the transient stability constraint as $|\delta_{UTMDM}(t_{LOSP}) - \delta_{CTMDM}(t_{LOSP})| \leq K_h$.

step 5: Solve TSC-OPF and obtain new operating point. Replace the BOP with TSC-OPF operating point. Go to step 2.

step 6: check for multi swing instability. If system is multi swing stable, go to step 9, otherwise go to step 7.

step 7: Determine rotor angle of each MDM at dynamic stationary point ($\delta_{MDMr}(t_{DSP})$), and form transient stability constraint as, $\delta_{MDM}(t_{DSP}) \leq \delta_{MDMr}(t_{DSP}) - \Delta$. Where, Δ is the desired deviation threshold to ensure multi swing stability.

step 8: Solve TSC-OPF and obtain new operating point. Replace the BOP with TSC-OPF operating point. Go to step 2.

step 9: Required control achieved, end the stabilization process.

V. NUMERICAL EXAMPLE AND DISCUSSION

The application of the proposed approach is demonstrated in this section using the scenario [TS, bus 11, 400 msec]. Simulations of TS are fully based on the system model presented in [19]. In the TSC-OPF problem, dynamic constraints are considered with a step limit of 0.01 s, and the TSC-OPF is solved using a MATLAB optimization solver which uses sequential quadratic programming for the optimization process.

The generating schedule at the base case operating point (IOP) is shown in Table 1. Individual machine kimbark curves are assessed to determine the transient stability for the contingency scenario considered at this IOP. Kimbark curves of machine-31 and machine-32 are shown in 5 (panel (a)). DLP happens on machine-31 at 0.49 s and machine-32 at 0.48 s, as can be shown in the figure. The presence of at least one DLP on post-fault kimbark curves, according to the unity principle, suggests the transient instability in the system. The rotor angle graphs also reveal that after the fault, these two machines begin to deviate from the rest of the system, resulting in overall system instability. The leading out of step point is obtained on machine-32 with $t_{LOSP} = 0.48$ s. Further, using the the procedure described in section III for the identification of MDM, for the considered contingency scenario, machine-32 is identified as MDM.

At the initial generation schedule, for the current contingency scenario, the system has CCT of 320 ms, such that

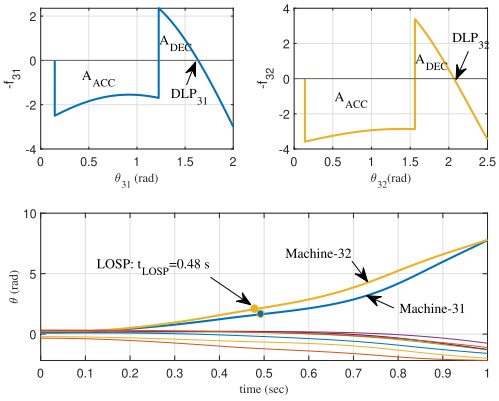

(a)

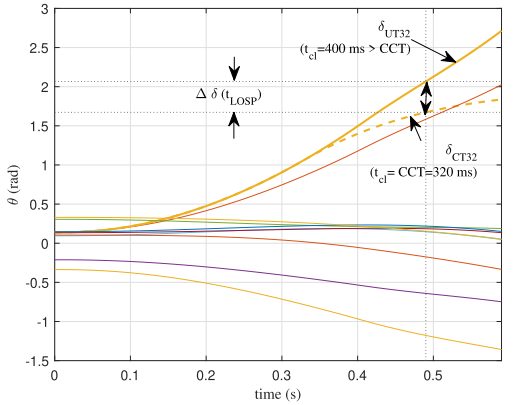

(b)

FIGURE 5. (a) Kimbark curves of machine-31 and 32 for the scenario [TS,bus-11,400 ms]. (b) Unstable and critical trajectory of MDM (machine-32) at the IOP for [TS,bus-11,400 ms].

TABLE 2. Generation schedule at OP_2 for [TS, bus-11, 400 ms].

Unit no	Power (MW)	Unit no	Power (MW)
Machine- 30	272.21	Machine- 35	652.55
Machine- 31	526.93	Machine- 36	547.76
Machine- 32	593.39	Machine- 37	564.24
Machine- 33	641.03	Machine- 38	878.44
Machine- 34	434.02	Machine- 39	1083.37
operating cost =62030 $/hr			

the critical trajectory of MDM has an angle deviation of $\delta_{CT32}(t_{LOSP}) = 1.6721$ rad, as shown in Fig. 5(panel(b)). Using this information about $\delta_{CT32}(t_{LOSP})$, the transient stability constraint in Eq.(6b) is included into TSC-OPF, and the solution of which yields second operating point OP_2 with corresponding generation schedule shown in Table 2.

At this operating point OP_2, system is again subjected to the same contingency and system is assessed unstable, as shown in Fig. 6. Again, leading LOSP occurs on machine-32 at time, $t_{LOSP} = 0.58$ s. It is interesting to note that at this new operating point, OP_2, the system time to instability is increased to 0.58 s from 0.48 s at the IOP,

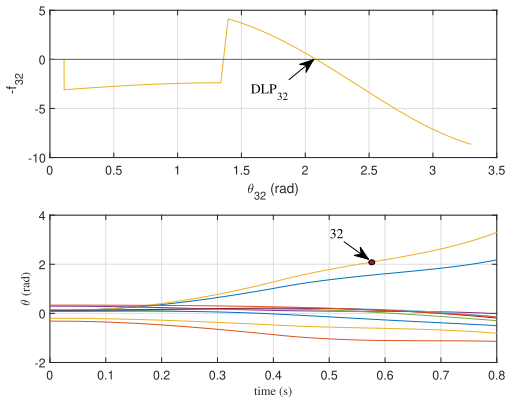

FIGURE 6. Machine-32 kimbark curve and rotor angle trajectories for the first iteration of TSC-OPF procedure. The system is unstable at OP_2.

TABLE 3. Generation schedule at OP_3 for [TS, bus-11, 400 ms].

Unit no	Power (MW)	Unit no	Power (MW)
Machine- 30	276.50	Machine- 35	658.42
Machine- 31	504.01	Machine- 36	552.99
Machine- 32	565.39	Machine- 37	570.24
Machine- 33	646.89	Machine- 38	886.97
Machine- 34	435.42	Machine- 39	1097.94
operating cost =62129 $/hr			

which is manifested in the form of improved system CCT from 0.32 s at the IOP to 0.36 s at OP_2. At OP_2 the critical trajectory of MDM has an angle deviation of $\delta_{CT32}(t_{LOSP}) = 1.7609$ rad. Using this information, again the transient stability constraint in Eq.(6b) is adjusted, and TSC-OPF is solved for new operating schedule OP_3. Table 3 shows the new generation schedule at OP_3. At this new operating schedule, the system again subjected to the considered contingency and the resulting system response is depicted in Fig.7. From the figure it can be easily seen that, the system is first swing stable but multi swing unstable. Further, with respect to first swing the CCT at OP_3 comes out to be 400 ms. Since, the system is first swing stable, there exists a dynamic stationary point (DSP) on the Kimbark curve of machine-32, and for the considered case it comes out to be $t_{DSP} = 0.85$ s and $\delta_{32r}(t_{DSP}) = 2.0493$ rad.

Now, to make system multi swing stable, transient stability constraint is formed as follows:

$$\delta_{32}(t_{DSP}) \leq \delta_{32r}(t_{DSP}) - \Delta. \tag{7}$$

Where, the parameter Δ is chosen by trail and hit method. For the considered case study, a value of $\Delta = 0.2$ rad has been chosen. Thus formed transient stability constraint is included in the TSC-OPF formulation and solved for new operating point, OP_4. Generation schedule at OP_4 is shown in Table 4. At this new generation schedule system is subjected to same contingency and corresponding plots are shown in Fig.8. It can be seen in the figure that only DSPs appears on the Kimbark curve of MDM-32 in successive swings,

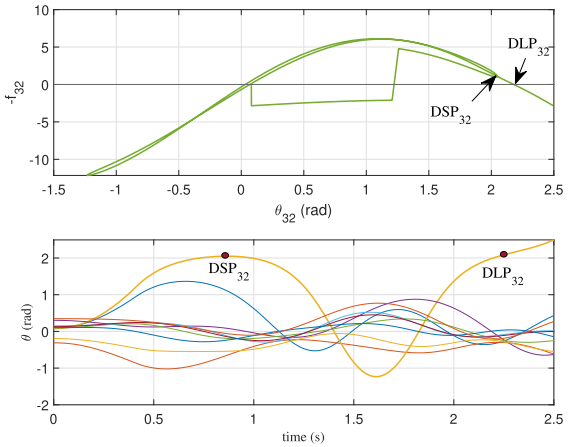

FIGURE 7. Machine-32 kimbark curve and rotor angle trajectories for the second iteration of TSC-OPF procedure. The system shows multi-swing instability at OP_3.

TABLE 4. Generation schedule at OP_4 for [TS, bus-11, 400 ms].

Unit no	Power (MW)	Unit no	Power (MW)
Machine- 30	278.28	Machine- 35	660.07
Machine- 31	486.15	Machine- 36	554.42
Machine- 32	435.74	Machine- 37	572.41
Machine- 33	648.86	Machine- 38	889.64
Machine- 34	435.74	Machine- 39	1104.91
operating cost =62177 $/hr			

showing that the MDM has stabilised for multiple swings. Corresponding rotor angle deviations plot also tells that once the MDM is stabilized all other machines also gets stabilized and hence system is transiently secured for the considered contingency.

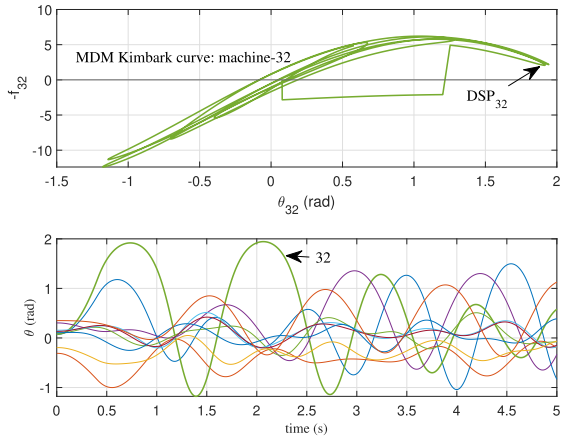

FIGURE 8. Machine-32 kimbark curve and rotor angle trajectories for the third and last iteration of TSC-OPF procedure. The system is stable at OP_4.

The proposed approach, at the operating point, OP_4, improves the system CCT to 405 ms, which is just 1.25% above the actual fault duration, which means the system is critically stabilized for the considered contingency.

Fig.9 (panel (a)) shows the variation of MDM stability margin with respect to TSC-OPF iterations to stabilize the

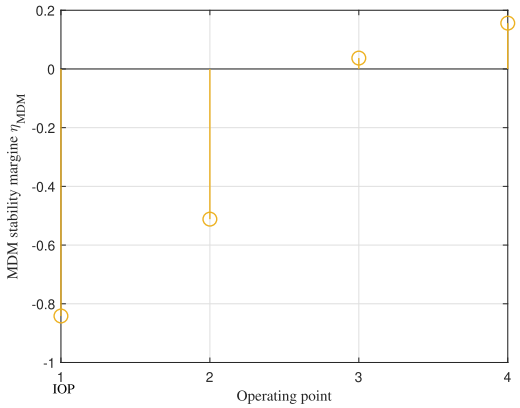

(a)

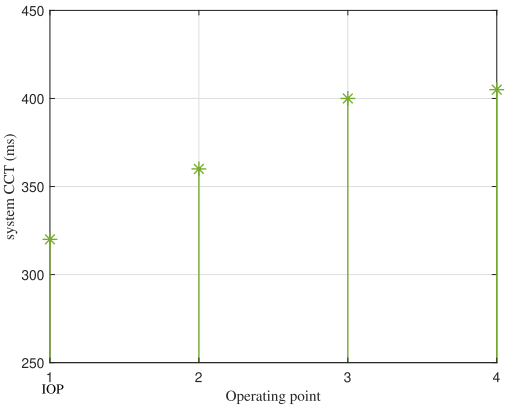

(b)

FIGURE 9. (a) Variation of MDM stability margin with respect to TSC-OPF iterations for contigency stabilization. (b) Variation of system CCT with respect to TSC-OPF iterations during contigency stabilization Variation of MDM stability margin and system CCT.

given contingency. The figure shows that MDM has a negative margin of -0.8146 at the IOP (stability margins are evaluated using the Eqs.(4a)-(4b), at the second iteration its stability margin is still negative but improved by approximately 39.21% over initial stability margin. For the third iteration MDM stability has small positive margin indicating that system is stable during first swing but will not ensure multi swing stability since there occurs DLP on MDM kimbark curve in the second swing. At the fourth iteration MDM margin becomes more positive (increased by 15.61% above the critical stability margin) and ensures that the system is both first swing and multi swing stable. Fig.9 (panel (b)) shows the variation of system CCT with respect to TSC-OPF iterations. Figure reveals that there exist a positive relation between system CCT and MDM stability margin, as increase in MDM stability margin resulting in increase of overall system CCT. Further, it is worth to point out here that for a given contingency system CCT can be adjusted easily by adjusting the value of parameter "Δ" in the proposed method. Because, the parameter "Δ" indirectly controls the amplitude of MDM

TABLE 5. Operating cost comparison.

Parameter	Proposed	Ref. [13]	Ref. [14]	Ref. [27]
Operating cost ($/hr)	60908.0	60916.8	61148.0	60908.0
CCT (ms)	102.00	107.10	159.00	102.00

first swing, so the larger value of "Δ" restricts the first swing rotor angle to a low value, which results in more secure operation of the system (i.e higher margins and CCT), where as lower values of "Δ" results in larger amplitudes in the first swing of MDM rotor angles, and hence results in less secure operation (i.e lower margins).

VI. COMPARISON WITH EXISTING APPROACHES

Table 6 compares the proposed transient stability control approach with the existing approaches. The proposed control approach, needs to incorporate TSC just as many as number of MDMs, N_{MDM}. Only one time step, t_{LOSP}, is used to enforce these constraints. Since for the given fault scenario MDMs are only small fraction of total number of generators [27], number of TSC in the current method are always lesser compared to [5]. Even though, in [13], TSC number is decreased to one by using single machine equivalent SIME) approach, as SIME approach relies on aggregation of multi machine trajectory dynamics into one machine equivalent, results in non negligible approximation errors. Further, in [13],TSC-OPF solution period end time(i.e t_{end}) is set to, t_u, SIME trajectory time to instability. This necessitates the use of a separate computer application to merge SIME calculations with time domain simulations. However, for the approach presented in this paper, t_{end} is determined as time to leading out of step point, t_{LOSP}, which is obtained directly from the individual machines kimbark curves.

The following case study from the 39 bus 10 machine system is used to compare the suggested method to existing methods in terms of operating cost. The case investigated is a three-phase ground fault at bus 29, which is cleared by tripping the line between buses 26 and 29. The same case study was presented in [14] and in [13] [section VIII-B]. Machine-38 is the MDM in this example.The final operating cost and CCT from the proposed technique are shown in Table 5.

As the scenario in hand leads to only first-swing instability, the proposed technique and [27] which adopts the transient stability constraints based on MDM trajectories achieves near-critical system operation for the considered contingency, resulting in low operating costs. With a CCT of just 2% above the actual fault clearance time, the proposed solution has a low operational cost while assuring system stability. For the same contingency, [13] has achieved only the minimal CCT which is 7% higher than the actual fault duration, hence the operating cost achieved is higher than the method presented in this paper. In [14], a less optimum but more secure system operation is achieved. This reason being the consideration of a low value for the heuristic TSC, which resulted in over

TABLE 6. Proposed approach comparison with existing approaches.

Parameter	Ref. [5], [14]	Ref. [13]	Ref. [27]	Proposed
TSC-OPF integration interval end time t_{end}	Arbitrary t_{end}	Not arbitrary t_u	Not arbitrary $\boldsymbol{t_{end} \geq t_{end}^{emp}}$	**Not arbitrary** $\boldsymbol{t_{LOSP}}$
TSC-OPF time steps number	Arbitrary $N_a = (t_{end} - t_0)/\Delta t$	Not arbitrary $N_b = (t_u - t_0)/\Delta t$	Not arbitrary $N_c = (t_{end} - t_0)/\Delta t$	**Not arbitrary** $N_d = (t_{LOSP} - t_0)/\Delta t$
Number of Transient stability constraints	$N_g{*}N_a$ N_g: number of generators	1	$N_{MDM} * N_c$ N_{MDM}: number of MDMs	$\boldsymbol{N_{MDM}}$ N_{MDM}: number of MDMs
Number of generator dynamic constraints	$2N_g{*}N_a$	$2N_g{*}N_b$	$2N_g{*}N_c$	$\boldsymbol{2N_g{*}N_d}$
Heuristic stability criterion	Yes	No	No	**No**
Iterative procedure	No	Yes	No	**Yes**
Derivation of single machine equivalent trajectory	No	Yes	No	**No**

compensated operation i.e., system critical clearing time is 59% higher than the actual fault duration. In addition (see Table 6), if the TSC-OPF solution period for the current scenario is defined arbitrarily as,$t_{end} = 1.5$ s, time to instability from SIME comes as $t_u = 0.5$ s, and time to leading out of step point, t_{LOSP} from the proposed method comes as 0.44 s, the number of generator dynamic constraints plus TSC from the proposed method, in [5], [13], for a time step $\Delta t = 0.01$ s comes out to be, 881, 4500, and 1001 respectively.

VII. DISCUSSION ON SOME ASPECTS OF THE PROPOSED METHOD W.R.T [27]

1). In [27], to form transient stability constraint, critical trajectory of MDM at only initial operation point is used, and then this constraint is adjusted non heuristically by choosing a suitable value for severity index,γ_{MDM}. Once selected, transient stability constraint is fixed for entire solution process and included for all time steps of solution in optimization problem, and while solving the optimization problem this constraint may affect the rotor angle solution at some time steps and does not affect the rotor angle solution at some other time steps. In other words, even though we are applying this constraint for all time steps of solution, it may not be active constraint for the solution at certain time steps. Whereas, in the present paper, transient stability constraints are still formed from the critical trajectories of MDM, but these critical trajectories do not correspond to any fixed operating point. As the iteration progress, the operating point improves, and critical trajectories at each improved operating point is further utilized in forming the transient stability constraint. Since, the transient stability constraint is formed in terms of critical trajectories of MDM at improved operating point, this better represents the dynamic response of the power system compared to transient stability constraints in [27].

2). In [27], a non-iterative technique of TSC-OPF with transient stability constraints included at all time steps of solution interval, and dynamic constraints included for a time interval $[t_0\ t_{end}^{emp}]$, is proposed. Where, t_{end}^{emp}, is just an empirical time limit which is defined completely based on numerous simulation studies experience. In the present paper, an iterative process of TSC-OPF inspired from [13] is explored from the sense of individual machines for the first time. As mentioned in [23], IMEAC based method identifies transient instability quickly than EEAC/SIME based methods, as time to leading loss of synchronism point(t_{LOSP}) is less than the time to instability of SIME trajectory (t_u). So, forming transient stability constraints in terms of individual machines offers to advantages (i). Eliminates the need of resorting to any multi machine to one machine equivalent transformations to reduce number of transient stability constraints (ii). As, $t_{LOSP} < t_u$, time for which dynamic constraints need to be included in the optimization problem gets reduced, which results in less number dynamic constraints.

3). The main computational burden of TSC-OPF comes from the dynamic constraints. The computational burden added by transient constraints is relatively not significant as far as the solver's operation is considered. But, it is still advantageous to come up with minimal set of transient constraints that can be used in TSC-OPF for a given contingency stabilization. In this process, Ref. [27] which is the starting paper to explore this IMEAC in transient control, come up with an initial idea of forming transient stability constraints for all time steps in terms of MDM critical trajectories at the initial operating point. The idea of utilizing MDM trajectories is further refined in the present paper such that only one transient stability constraint at one time step is formed and it is always acts as an active constraint in the optimization problem. Further,the authors acknowledge that Ref. [13] is the source of inspiration for this improvement.

To demonstrate the differences and relevant advantages of the proposal with respect to the work in [27], let us considered scenario [TS, bus 4, 400 ms, line 4-5], which is a three phase to ground fault at bus 4 in test system and cleared after 400 ms by tripping the line connected between buses 4 and 5. This is the same case study presented in [section VI (1)] of [27]. For the case in hand machine connected to bus-31

TABLE 7. Size comparison of proposed approach with that of [27] while stabilizing a representative contingency scenario [TS, bus 4,400 ms, line 4-5].

Parameter	Ref. [27]	Proposed
TSC-OPF integration interval end time t_{end}	$t_{end} \geq t_{end}^{emp}$=1.08 s	$\boldsymbol{t_{end} = t_{LOSP}}$ =0.58 s
TSC-OPF time steps number	$N_c \geq 108$	$N_d = 58$
Number of Transient-stability constraints	$N_{MDM} * N_c \geq$108	$\boldsymbol{N_{MDM}}$=1
Number of generator-dynamic constraints	$2N_g{*}N_c \geq 2*10*108$ $\geq$2160	$\boldsymbol{2N_g{*}N_d}$ =2*10*58 =1160
Number of TSC-OPF-runs for stabilizing the contingency.	1	2

is the only MDM. The following table briefly summarizes the computational parameters involved in both the methods while stabilizing this contingency.

From the Table 7 it can be observed that, for stabilizing the case in hand using the method in [27], TSC-OPF needs to be solved for an minimum empirical time of 108 s, which resulted into at least 108 transient stability constraints and 2160 dynamic constraints. Whereas in the proposed method, since TSC-OPF solution interval is defined as t_{LOSP}, which is very less compared to t_{end}^{emp} of [27], TSC-OPF needs to be solved for only 0.58 s, which is associated with only one transient stability constraint, and 1160 dynamic constraints. However, it is worth to note at this point that, method proposed in [27] is a non-iterative process i.e optimal generation schedule is obtained by solving TSC-OPF once with large number transient and dynamic constraints. Whereas, the proposed method reschedules the generation optimally while stabilizing the given contingency in two iterations, where in each iteration the constraints size of optimization problem is reduced considerably compared to [27].

The main objective of the present paper and [27] is to explore the potential of IMEAC based TSA theory, for transient stability control through TSC-OPF. However, authors would like to emphasize at this point that, the proposed method cannot be seen as a substitute for existing methods of forming transient stability constraints but can be seen as a distinctive way of explaining the formation of transient stability constraints (both dynamic and transient constraints) in TSC-OPF from the individual machine analysis. Two possible ways for achieving this objective are presented independently in [27], and in the present paper.

VIII. CONCLUSION

A transient stability enhancement approach through transient stability constrained optimal power flow is presented in this study. Transient stability constraints (TSC) in this proposed technique are formed directly using the unstable and critical trajectories of some selective individual machines called most disturbed machines (MDM). The important aspects of proposed technique can be summarized as follows:

(i). The TSC is formed using the reference trajectory of MDM at single time step. This formulation makes the dimension of TSC equals to simply number of MDMs for the given contingency.

(ii). The length of time domain simulations that needs to be discretized for forming dynamic constraints in TSC-OPF is limited for a time called time to leading out of step point, t_{LOSP}, which is the time at which the transient instability is detected first time on mulitimachine trajectories. In addition, as the proposed TSC is formulated using the reference trajectories of MDM, the system operation is not limited by a fixed value of TSC, but adjusted w.r.t to the TSC that actually represents the powersystem dynamic response more closely.

REFERENCES

[1] Y. Xu, Z. Y. Dong, Z. Xu, R. Zhang, and K. P. Wong, "Power system transient stability-constrained optimal power flow: A comprehensive review," in *Proc. IEEE Power Energy Soc. Gen. Meeting*, Jul. 2012, pp. 1–7, doi: 10.1109/PESGM.2012.6344753.

[2] G. Geng, S. Abhyankar, X. Wang, and V. Dinavahi, "Solution techniques for transient stability-constrained optimal power flow—Part I," *IET Gener. Transmiss. Distrib.*, vol. 11, no. 12, pp. 3177–3185, Aug. 2017.

[3] L. Chen, Y. Taka, H. Okamoto, R. Tanabe, and A. Ono, "Optimal operation solutions of power systems with transient stability constraints," *IEEE Trans. Circuits Syst. I, Fundam. Theory Appl.*, vol. 48, no. 3, pp. 327–339, Mar. 2001.

[4] X. Tong, C. Ling, and L. Qi, "A semi-infinite programming algorithm for solving optimal power flow with transient stability constraints," *J. Comput. Appl. Math.*, vol. 217, no. 2, pp. 432–447, 2008.

[5] D. Gan, R. J. Thomas, and R. D. Zimmerman, "Stability-constrained optimal power flow," *IEEE Trans. Power Syst.*, vol. 15, no. 2, pp. 535–540, May 2000.

[6] Y. Yuan, J. Kubokawa, and H. Sasaki, "A solution of optimal power flow with multicontingency transient stability constraints," *IEEE Trans. Power Syst.*, vol. 18, no. 3, pp. 1094–1102, Aug. 2003.

[7] I. A. Calle, E. D. Castronuovo, and P. Ledesma, "Optimal re-dispatch of an isolated system considering transient stability constraints," *Int. J. Electr. Power Energy Syst.*, vol. 44, no. 1, pp. 728–735, Jan. 2013.

[8] P. Ledesma, I. A. Calle, E. D. Castronuovo, and F. Arredondo, "Multi-contingency TSCOPF based on full-system simulation," *IET Gener., Transmiss. Distrib.*, vol. 11, no. 1, pp. 64–72, Jan. 2017.

[9] I. A. Calle, P. Ledesma, and E. D. Castronuovo, "Advanced application of transient stability constrained-optimal power flow to a transmission system including an HVDC-LCC link," *IET Gener., Transmiss. Distrib.*, vol. 9, no. 13, pp. 1765–1772, Oct. 2015.

[10] Y. Xia and K. W. Chan, "Dynamic constrained optimal power flow using semi-infinite programming," *IEEE Trans. Power Syst.*, vol. 21, no. 3, pp. 1455–1457, Aug. 2006.

[11] M. La Scala, M. Trovato, and C. Antonelli, "On-line dynamic preventive control: An algorithm for transient security dispatch," *IEEE Trans. Power Syst.*, vol. 13, no. 2, pp. 601–610, May 1998.

[12] R. Zarate-Minano, T. Van Cutsem, F. Milano, and A. J. Conejo, "Securing transient stability using time-domain simulations within an optimal power flow," *IEEE Trans. Power Syst.*, vol. 25, no. 1, pp. 243–253, Feb. 2010, doi: 10.1109/TPWRS.2009.2030369.

[13] A. Pizano-Martianez, C. R. Fuerte-Esquivel, and D. Ruiz-Vega, "Global transient stability-constrained optimal power flow using an OMIB reference trajectory," *IEEE Trans. Power Syst.*, vol. 25, no. 1, pp. 392–403, Feb. 2010.

[14] D. Layden and B. Jeyasurya, "Integrating security constraints in optimal power flow studies," in *Proc. IEEE Power Eng. Soc. Gen. Meeting*, Jun. 2004, pp. 125–129.

[15] S. Xia, Z. Ding, M. Shahidehpour, K. W. Chan, S. Bu, and G. Li, "Transient stability-constrained optimal power flow calculation with extremely unstable conditions using energy sensitivity method," *IEEE Trans. Power Syst.*, vol. 36, no. 1, pp. 355–365, Jan. 2021.
[16] H. Nguyen-Duc, L. Tran-Hoai, and D. Vo Ngoc, "A novel approach to solve transient stability constrained optimal power flow problems," *Turkish J. Elect. Eng. Comput. Sci.*, vol. 25, no. 6, pp. 4696–4705, 2017, doi: 10.3906/elk-1704-209.
[17] A. A. Fouad and S. E. Stanton, "Transient stability of a multi-machine power system part I: Investigation of system trajectories," *IEEE Trans. Power App. Syst.*, vol. PAS-100, no. 7, pp. 3408–3416, Jul. 1981, doi: 10.1109/TPAS.1981.316683.
[18] A. A. Fouad and S. E. Stanton, "Transient stability of a multi-machine power system. Part II: Critical transient energy," *IEEE Trans. Power App. Syst.*, vol. PAS-100, no. 7, pp. 3417–3424, Jul. 1981, doi: 10.1109/TPAS.1981.316684.
[19] A. Michel, A. Fouad, and V. Vittal, "Power system transient stability using individual machine energy functions," *IEEE Trans. Circuits Syst.*, vol. CS-30, no. 5, pp. 266–276, May 1983.
[20] S. E. Stanton and W. P. Dykas, "Analysis of a local transient control action by partial energy functions," *IEEE Trans. Power Syst.*, vol. 4, no. 3, pp. 996–1002, Aug. 1989.
[21] S. E. Stanton, "Transient stability monitoring for electric power systems using a partial energy function," *IEEE Trans. Power Syst.*, vol. 4, no. 4, pp. 1389–1396, Nov. 1989.
[22] S. Wang, J. Yu, and W. Zhang, "Transient stability assessment using individual machine equal area criterion PART I: Unity principle," *IEEE Access*, vol. 6, pp. 77065–77076, 2018.
[23] S. Wang, J. Yu, and W. Zhang, "Transient stability assessment using individual machine equal area criterion Part II: Stability margin," *IEEE Access*, vol. 6, pp. 38693–38705, 2018.
[24] S. Wang, J. Yu, and W. Zhang, "Transient stability assessment using individual machine equal area criterion PART III: Reference machine," *IEEE Access*, vol. 7, pp. 80174–80193, 2019.
[25] S. Wang, J. Yu, A. M. Foley, and W. Zhang, "Transient energy of an individual machine PART I: Stability characterization," *IEEE Access*, vol. 9, pp. 44797–44812, 2021.
[26] S. Wang, J. Yu, A. M. Foley, and W. Zhang, "Transient energy of an individual machine PART II: Potential energy surface," *IEEE Access*, vol. 9, pp. 60223–60243, 2021.
[27] S. Batchu and K. Teeparthi, "A preventive transient stability control strategy through individual machine equal area criterion framework," *IEEE Access*, vol. 9, pp. 167776–167794, 2021.
[28] M. A. Pai, *Energy Function Analysis for Power System Stability*. Norwell, MA, USA: Kluwer, 1989.
[29] T. B. Nguyen and M. A. Pai, "Dynamic security-constrained rescheduling of power systems using trajectory sensitivities," *IEEE Trans. Power Syst.*, vol. 18, no. 2, pp. 848–854, May 2003.

SREENADH BATCHU was born in Krishna, Andhra Pradesh, India, in 1989. He received the B.Tech. degree in electrical and electronics engineering from Jawaharlal Nehru Technological University Kakinada, India, in 2010, and the M.Tech. degree in power and energy system from the National Institute of Technology Karnataka, India, in 2012. He is currently pursuing the Ph.D. degree with the Department of Electrical Engineering, National Institute of Technology Andhra Pradesh, India.

Since 2019, he has been an Assistant Professor with the Electrical Engineering Department, RGUKT Nuzvid, Andhra Pradesh. His research interests include power system dynamic security assessment and control.

KIRAN TEEPARTHI (Member, IEEE) was born in Andhra Pradesh, India. He received the B.E. degree in electrical and electronics engineering from Andhra University, India, the M.Tech. degree in power systems from the National Institute of Technology Jamshedpur, India, and the Ph.D. degree in electrical engineering from the National Institute of Technology Warangal, India.

Since 2019, he has been an Assistant Professor with the Electrical Engineering Department, NIT Andhra Pradesh. His current research interests include power system security and stability, power system operation and control, renewable energy integration issues, power system optimization, and artificial intelligence (AI) applications to power systems.